

# SCIENTIFIC REPORTS



OPEN

## Thermodynamic Calculation among Cerium, Oxygen, and Sulfur in Liquid Iron

Fei Pan<sup>1,2,3,\*</sup>, Jian Zhang<sup>1,4,\*</sup>, Hao-Long Chen<sup>5</sup>, Yen-Hsun Su<sup>1</sup>, Yen-Hao Su<sup>6</sup> & Weng-Sing Hwang<sup>1</sup>

Received: 25 May 2016

Accepted: 06 October 2016

Published: 21 October 2016

Thermodynamic calculation has been applied to predict the inclusion formation in molten SS400 steel. When the Cerium addition in liquid iron is 70 ppm and the initial Oxygen and Sulphur are both 110 ppm, the formation of oxides containing Cerium would experience the transformation from  $Ce_2O_3$  to  $CeO_2$  and also the formation of sulfides containing Cerium would experience the transformation from  $CeS$  to  $Ce_2S_3$  and then to  $Ce_3S_4$ . Below 2000 K the most thermodynamic stable matter is  $CeO_2$  and the less thermodynamic stable inclusion is  $CeS$ . Only when the amount of [O] is extremely low and the amount of [S] and [Ce] is relatively high,  $Ce_2S_3$  has the possibility to form.

Rare earth (RE) metals have many applications<sup>1–5</sup> and their addition to molten iron has attracted increasing research attention<sup>6</sup>. Such addition affects inclusion structures<sup>7</sup> and can be used to purify steel<sup>8</sup>. The conjugation between oxygen and RE metals<sup>9</sup> and between sulfur and RE metals<sup>10</sup> is very strong. A lot of research<sup>11–13</sup> has been done on the equilibrium relation between O, S, and RE metals. It has been found that extremely low oxygen and sulfur concentrations in steel can be achieved via the addition of an RE metal<sup>14</sup>. A lot of research<sup>15–18</sup> has also been done on steel deoxidization and desulfurization via titanium and magnesium. RE metals can be used to deoxidize and desulfurize steel to control inclusion size and chemical composition. Few studies have performed thermodynamic calculations on the use of cerium to modify inclusions.

This paper focuses on the thermodynamic calculations of the cerium-oxygen-sulfur system in molten SS400 steel. The formation conditions of  $CeS$ ,  $Ce_2S_3$ ,  $Ce_3S_4$ ,  $CeO_2$ , and  $Ce_2O_3$  in molten steel are examined using Wagner's relation and Lupis's relation based on the Gibbs free energy change. The transformation mechanism is analyzed by determining the thermodynamic conditions of Ce-desulfurized and Ce-deoxidized steel. The segregation of  $Ce_2O_3$  in molten iron is also analyzed. In addition, a model for predicting the formation of various inclusions is established for SS400 steel with cerium addition.

### Calculations

The thermodynamic calculations of the Ce-O-S system are based on Wagner's relation<sup>19</sup> and Lupis' relation<sup>20</sup>. These calculations were implemented in C++. The segregation of  $Ce_2O_3$  in molten SS400 steel, whose chemical composition is shown in Table 1, was calculated in Matlab 2015a.

The Ce-O-S system is the thermodynamic relation between the dissolved Oxygen, Sulphur and Cerium in liquid iron to explore the formations of inclusions containing Cerium. The first stage for thermodynamic calculation is to derive the thermodynamic equations for the inclusion formations by Wagner's relation<sup>19</sup> and Lupis' relation<sup>20</sup>. Then the second stage is to use C++ programming software to derive the unknown chemical composition values for every equation.

### Results and Discussion

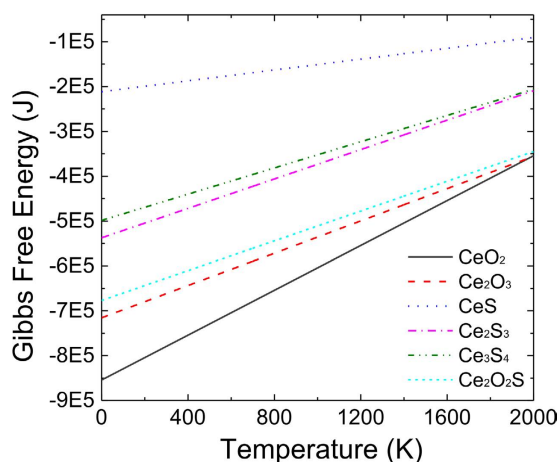
For the addition of cerium into molten SS400 steel, the reactions of [O], [S], and [Ce] are of interest because Ce has strong affinity with S and O. As reported previously<sup>21</sup>, when  $w(CE)/(w[O] + w[S]) = 3.9$ , the function of

<sup>1</sup>Department of Materials Science and Engineering, National Cheng Kung University, Tainan 70101, Taiwan. <sup>2</sup>Physics Department, Technische Universität München, Munich 85748, Germany. <sup>3</sup>Physics Department, Ludwig-Maximilians-Universität München, Munich 80799, Germany. <sup>4</sup>Chengdu Base, Panzhihua Iron & Steel Research Institute Co., LTD, Chengdu 610399, China. <sup>5</sup>Department of Electronic Engineering, Kao Yuan University, Kaohsiung 82151, Taiwan. <sup>6</sup>Steelmaking Process Development Section, China Steel Corporation, Kaohsiung 81233, Taiwan. \*These authors contributed equally to this work. Correspondence and requests for materials should be addressed to F.P. (email: phoenix.pan@tum.de) or W.-S.H. (email: wshwang@mail.ncku.edu.tw)

C	Si	Mn	P	S	O
0.14	0.26	0.90	0.02	0.03	0.018

**Table 1. Chemical composition of SS400 steel (wt. %).**

Reaction	Standard Gibbs Free energy, J/mol	No.
[Ce] + 2[O] = CeO <sub>2</sub> (s)	$\Delta G^\theta = -854270 + 250T$	(3)
[Ce] + 3/2[O] = 1/2Ce <sub>2</sub> O <sub>3</sub> (s)	$\Delta G^\theta = -715560 + 180T$	(4)
[Ce] + [S] = CeS(s)	$\Delta G^\theta = -211390 + 60.5T$	(5)
[Ce] + 3/2[S] = 1/2Ce <sub>2</sub> S <sub>3</sub> (s)	$\Delta G^\theta = -537290 + 164T$	(6)
[Ce] + 4/3[S] = 1/3Ce <sub>3</sub> S <sub>4</sub> (s)	$\Delta G^\theta = -498480 + 146.3T$	(7)
[Ce] + [O] + 1/2[S] = 1/2Ce <sub>2</sub> O <sub>2</sub> S(s)	$\Delta G^\theta = -676795 + 166T^{18}$	(8)

**Table 2. Formation equations and Gibbs free energy of oxides, sulfides and oxysulfides of cerium<sup>14,21–26</sup>.****Figure 1. Gibbs free energy of formation for various oxides and sulfides containing cerium at various temperatures.**

cerium is optimal. To determine the separation sequence for various oxides and sulfides of cerium, the amount of cerium in the calculations was set as 1 mol to compare the Gibbs free energy of formation for various inclusions, which can be derived as:

$$\Delta G = \Delta G^\theta + RT \ln J \quad (1)$$

$$\Delta G^\theta = -RT \ln K \quad (2)$$

where  $J$  denotes the reaction quotient (unitless),  $\Delta G$  is the Gibbs free energy change of reaction (J/mol),  $\Delta G^\theta$  denotes the Gibbs free energy change of reaction for unmixed reactants and products at standard conditions (J/mol),  $R$  is the gas constant ( $\text{J}\cdot\text{mol}^{-1}\cdot\text{K}^{-1}$ ),  $T$  is temperature (K), and  $K$  is the equilibrium constant (unitless).

The Gibbs free energy of oxides, sulfides and oxysulfides of cerium are shown in Table 2<sup>14,21–26</sup>.

Below 2000 K, the most thermodynamically stable inclusion was CeO<sub>2</sub>, as shown in Fig. 1. Therefore, CeO<sub>2</sub> likely formed in the molten iron when the temperature reached the simulated steelmaking temperature of 1873 K. In Fig. 1, it could be read that the least thermodynamic stable inclusion is CeS and the thermodynamic stable sequence of the possible inclusion formed in liquid steel is CeO<sub>2</sub> > Ce<sub>2</sub>O<sub>3</sub> > Ce<sub>2</sub>O<sub>2</sub>S > Ce<sub>2</sub>S<sub>3</sub> > Ce<sub>3</sub>S<sub>4</sub> > CeS. However, the most thermodynamically stable matter does not guarantee the formation of CeO<sub>2</sub>, because the formation of oxides containing cerium are controlled not only by the equilibrium constant but also by the concentrations of cerium and oxygen in the molten iron. That is to say, the formation of CeO<sub>2</sub> at 1873 K is also determined by the solubility product of CeO<sub>2</sub> and the concentration of cerium and oxygen, even though the Gibbs Free Energy of CeO<sub>2</sub> is the lowest at 1873 K.

The activities and activity coefficient of Ce, O and S can be written as Eqs (9) and (10) from Wagner's relation<sup>7</sup> and Lupis' relation<sup>20</sup> as follow,

$$\alpha_i = f_i \cdot w[i] \quad (9)$$

$e_i^j$	$e_{Ce}^{Ce}$	$e_S^{Ce}$	$e_{Ce}^S$	$e_S^S$	$e_O^{Ce}$	$e_{Ce}^O$	$e_O^O$
T = 1873 K	0.0039	-9.1	-40	-0.046	-64	-560	-0.17

**Table 3.** First-order interaction parameter  $e_i^j$  of cerium, oxygen, and sulfur at 1873 K<sup>30</sup>.

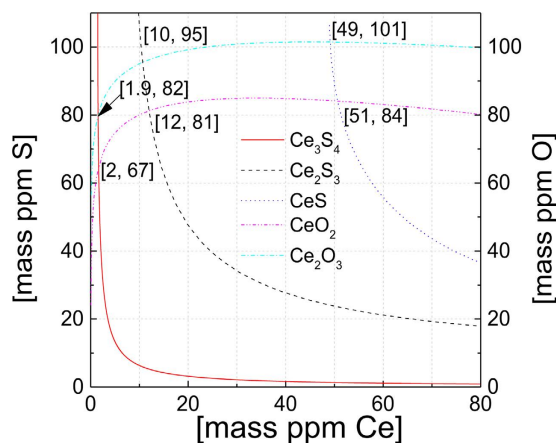


**Figure 2.** Deoxidation and Desulfurization with Cerium in liquid iron at 1873 K.

$$\lg f_i = \sum_j^n e_i^j w[j] \quad (10)$$

where  $f_i$  is the Henrian activity coefficient of component  $i$  relative to the dilute solution and  $e_i^j$  is the first-order interaction parameter of  $i$  on  $j$  in molten iron;  $w[i]$  and  $w[j]$  are the mass percentages of elements  $i$  and  $j$ , respectively (Table 3);  $\alpha_i$ ,  $s$  the activity of element  $i$ .

By using data<sup>22,23</sup> from Tables 2 and 3, the following curves for Ce-S and Ce-O in Fig. 2 can be calculated. The key to derive every line in Fig. 2 is the relation of equilibrium constant, Gibbs free energy and the amount of the chemical compositions for every possible inclusion according to Wagner's relation<sup>19</sup> and Lupis' relation<sup>20</sup>. When the equilibrium constant is linked to the amount of the chemical compositions for every possible inclusion, equations for Fig. 2 can be obtained. When the weight percentage of cerium, oxygen and sulphur are known in the molten iron at 1873 K, the main inclusion formed would be found in Fig. 2. As shown in Fig. 2, if the cerium addition in liquid iron is 70 ppm and the initial oxygen and sulphur are both 110 ppm, the formation of oxides containing cerium would experience the transformation from  $Ce_2O_3$  to  $CeO_2$  and also the formation of sulfides containing cerium would experience the transformation from  $CeS$  to  $Ce_2S_3$  and then to  $Ce_3S_4$ . From Fig. 2, when the temperature of molten iron reached 1873 K,  $Ce_3S_4$  is the main product, as the amount of cerium in molten iron is high and the amount of sulphur is relatively lower compared to the formation of  $CeS$  and  $Ce_2S_3$ .

In order to investigate the formation conditions of  $Ce_2O_3$ ,  $Ce_2S_3$  and  $Ce_2O_2S$ , the doubly saturated curve with  $Ce_2O_3/Ce_2O_2S$  and  $Ce_2S_3/Ce_2O_2S$  are calculated, using the thermodynamic data derived in Tables 2 and Equation 1–2.

In molten iron, it is assumed that  $K_{Ce_2O_3,1873K} = [\%Ce]^2 \cdot [\%O]^3 = 10^{-11}$  and  $K_{Ce_2S_3,1873K} = [\%Ce]^2 \cdot [\%S]^3 = 10^{-6}$ . Based on the reaction  $Ce_2O_2S + [O] = Ce_2O_3 + [S]$ , it is found that  $[\%S] = 10[\%O]$  when  $Ce_2O_2S$  and  $Ce_2O_3$  coexist. When  $Ce_2O_2S$  and  $Ce_2S_3$  coexist in molten iron, it is derived that  $[\%S] = 100[\%O]$ , based on the thermodynamic calculation of the reaction  $Ce_2S_3 + 2[O] = Ce_2O_2S + 2[S]$ . Figure 3 was derived from the above calculations. In Fig. 3, it can be concluded that  $Ce_2O_3$  and  $Ce_2O_2S$  can exist in molten iron in a wide amount range of  $[Ce]$ ,  $[O]$  and  $[S]$ . More importantly, only when the amount of  $[O]$  is extremely low and the amount of  $[S]$  and  $[Ce]$  is relatively high,  $Ce_2S_3$  has the possibility to form.

Cerium is a perfect deoxidizer and desulfurizer for steel purification. Compared with other elements, for example Aluminum, Titanium, Magnesium and Calcium<sup>27,28</sup>, which can also deoxidize and desulfurize, cerium can form a complex compound  $Ce_2O_2S$  which contains Oxygen and Sulphur together. The formation possibility of  $Ce_2O_2S$  has been verified by Hu's research<sup>29</sup> when they studied the effect of Ce addition on the C-Mn steel microstructure. It is reported by Wang<sup>26</sup> that  $Ce_2O_3$  is easier to form in molten iron when the iron molten temperature is 1873 K. However, the thermodynamic conditions were changed when the temperature decreases from 1873 K to solidus temperature. On the other hand, when the temperature of molten iron decreases to that at which solid steel starts to form, the cerium and oxygen in the molten iron begin to segregate. Their amounts are respectively:

$$W_{(Ce)} = W_{(Ce)_0} (1 - f_s)^{k_{Ce}-1}$$

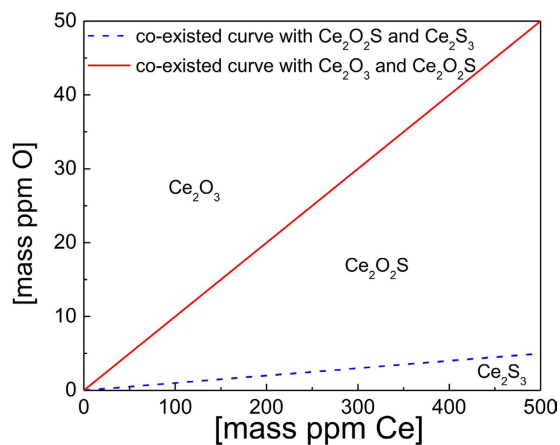


**Figure 3.** Relationship of [O] and [S] when  $\text{Ce}_2\text{O}_2\text{S}$ ,  $\text{Ce}_2\text{O}_3$ , and  $\text{Ce}_2\text{S}_3$  can form as stable compounds in molten iron at 1873 K.

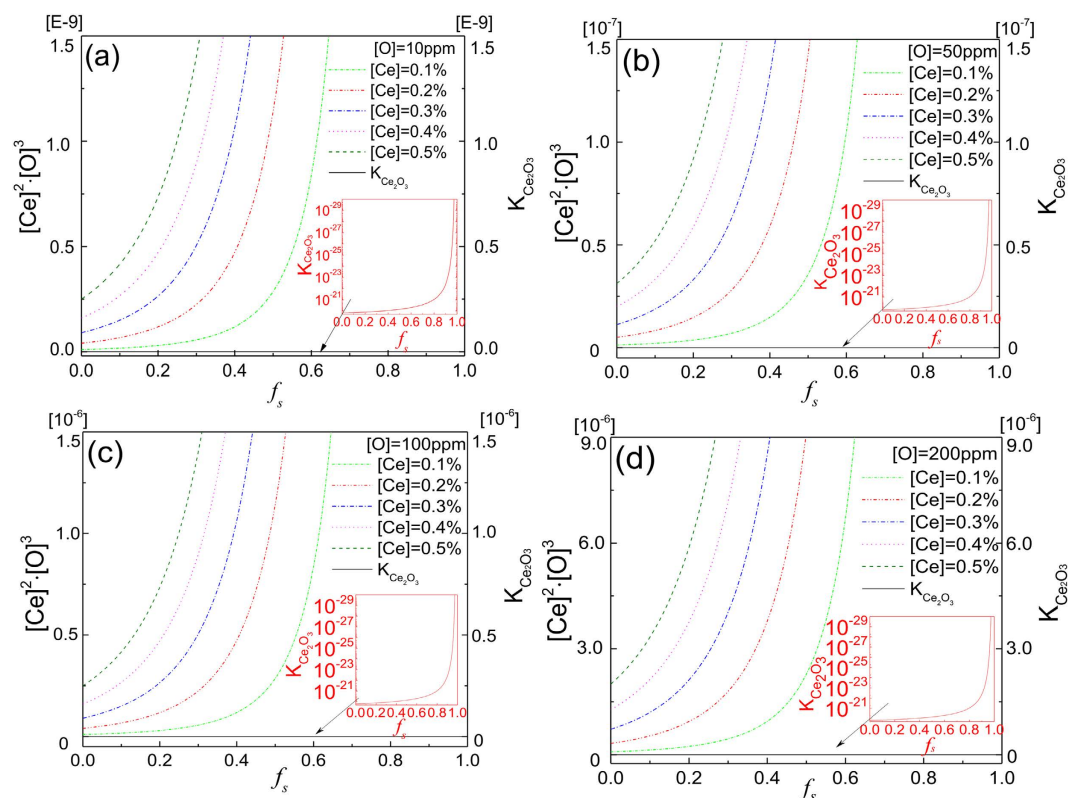


**Figure 4.** Segregation of  $\text{Ce}_2\text{O}_3$  in solid and liquid phases when  $\alpha_{[O]}$  is (a) 10, (b) 50, (c) 100, and (d) 200 ppm.

$$W_{(O)} = \frac{W_{(O)_0}}{f_s(k_0 - 1) + 1} \tag{12}$$

where  $W_{(Ce)}$  and  $W_{(O)}$  are the percentage amounts of cerium and oxygen of molten iron during the molten iron solidification, respectively;  $W_{(Ce)_0}$  and  $W_{(O)_0}$  are the initial percentage amounts of cerium and oxygen in the liquid phase, respectively;  $k_{Ce}$  ( $=0.005$ ) and  $k_O$  ( $=0.022$ ) are the solvent partition coefficients at equilibrium for cerium and oxygen, respectively;  $f_s$  is the solid fraction.

The solidus temperature of SS400 is 1777 K. The solubility product of the  $\text{Ce}_2\text{O}_3$  formed in molten iron can be expressed as:

$$Q_{\text{Ce}_2\text{O}_3} = W_{\text{Ce}}^2 \cdot W_{\text{O}}^3 \quad (13)$$

The solubility product of the  $\text{Ce}_2\text{O}_3$  formed in molten iron at equilibrium can be expressed as:

$$K_{\text{Ce}_2\text{O}_3} = \alpha_{\text{Ce}}^2 \cdot \alpha_{\text{O}}^3 = 10^{(-\frac{74695}{T} + 18.75)} \quad (14)$$

From Eqs (11) to (14), the solubility products versus solidification ratio ( $f_s$ ) are plotted in Fig. 4. In Fig. 4(a), where the simulated oxygen concentration in liquid steel is 10 ppm and the cerium concentration varies from 0.1% to 0.5%, the solubility products versus solidification ratio ( $f_s$ ) are plotted with the varying cerium concentration (shown in the colorful lines of Fig. 4(a)) and the equilibrium constant of  $\text{Ce}_2\text{O}_3$  ( $K_{\text{Ce}_2\text{O}_3}$ ) versus solidification ratio  $f_s$  is curved as the black solid line in Fig. 4(a). It is read in Fig. 4(a) that the colorful lines are all in the above of the black solid line, which means  $\text{Ce}_2\text{O}_3$  prefers to segregate in liquid phase with the 10 ppm Oxygen concentration in liquid iron. Moreover, the same conclusion can be drawn from the similar Fig. 4(b–d) with 50 ppm, 100 ppm, 200 ppm oxygen concentration in liquid iron. The inset red diagrams in Fig. 4(a–d) are the detailed solid black curves appeared in Fig. 4(a–d). Figure 4 shows that when the oxygen concentration in molten iron was increased from 10 to 200 ppm and the cerium concentration was in the range of 0.1% to 0.5%,  $\text{Ce}_2\text{O}_3$  preferred to segregate in the liquid phase.

## Conclusion

By the addition of cerium in molten SS400 steel, when the temperature of molten iron reached 1873 K, at the same time that the Cerium addition in liquid iron is 70 ppm and the initial Oxygen and Sulphur are both 110 ppm, the formation of oxides containing Cerium would experience the transformation from  $\text{Ce}_2\text{O}_3$  to  $\text{CeO}_2$  and also the formation of sulfides containing Cerium would experience the transformation from  $\text{CeS}$  to  $\text{Ce}_2\text{S}_3$  and then to  $\text{Ce}_3\text{S}_4$ . Below 2000 K the most thermodynamic stable matter  $\text{CeO}_2$  and the least thermodynamic stable inclusion is  $\text{CeS}$ . And the thermodynamic stable sequence of the possible inclusions formed in liquid steel is  $\text{CeO}_2 > \text{Ce}_2\text{O}_3 > \text{Ce}_2\text{O}_2\text{S} > \text{Ce}_2\text{S}_3 > \text{Ce}_3\text{S}_4 > \text{CeS}$ . Only when the amount of [O] is extremely low and the amount of [S] and [Ce] is relatively high,  $\text{Ce}_2\text{S}_3$  has the possibility to form. With the amount of oxygen in molten iron increasing from 10 ppm to 200 ppm and the amount range of cerium increasing from 0.1% to 0.5%,  $\text{Ce}_2\text{O}_3$  prefers to segregate in liquid phase all the time.

## References

- Su, Y. & Lai, Y. Performance enhancement of natural pigments on a high light transmission  $\text{ZrO}_2$  nanoparticle layer in a water-based dye-sensitized solar cell. *Int. J. Energ. Res.* **38**, 436–443 (2014).
- Kung, P. *et al.* Down-conversion photoluminescence sensitizing plasmonic silver nanoparticles on ZnO nanorods to generate hydrogen by water splitting photochemistry. *Appl. Phys. Lett.* **106**, 023114 (2015).
- Lin, K. & Su, Y. Photoluminescence of Cu: ZnS, Ag: ZnS, and Au: ZnS nanoparticles applied in Bio-LED. *Appl. Phys. B: Lasers Opt.* **113**, 351–359 (2013).
- Lai, Y., Su, Y. & Lin, M. Photochemical water splitting performance of Fluorescein, Rhodamine B, and Chlorophyll-Cu supported on  $\text{ZrO}_2$  nanoparticles layer anode. *Dyes Pigm.* **103**, 76–81 (2014).
- Su, Y. *et al.* Ellipsometric advances for local surface plasmon resonance to determine chitosan adsorption on layer-by-layer gold nanoparticles. *Appl. Spectrosc.* **61**, 1007–1014 (2007).
- Fruehan, R. J. The effect of zirconium, cerium, and lanthanum on the solubility of oxygen in liquid iron. *Metall. Mater. Trans. B*, **5**, 345–347 (1974).
- Wilson, W. G., Kay, D. & Vahed, A. The use of thermodynamics and phase equilibria to predict the behavior of the rare earth elements in steel. *J. O. M.* **26**, 14–23 (1975).
- Fischer, W. A. & Bertram, H. The deoxidation, desulphurization and nitrogen removal of iron melts containing oxygen, sulfur or nitrogen using the rare earth metals cerium and lanthanum. *Arch. Eisenhüttenwes.* **44**, 87–95 (1973).
- Han, Q. *et al.* Equilibria between cerium or neodymium and oxygen in molten iron. *Metall. Mater. Trans. B* **21**, 295–302 (1990).
- Langenberg, F. C. & Chipman, J. Equilibrium between cerium and sulfur in liquid iron. *Trans. Met. Soc. AIME* **212**, 290–293 (1958).
- Pan, F. *et al.* Effects of rare earth metals on steel microstructures. *Materials* **9**, 417 (2016).
- Arunachalam, V. & Ramachandran, S. Rare earths in steel technology. *Sci. Technol. Rare Earth Mater.* 415–434 (1980).
- Wu, Y., Wang, L. & Du, T. Thermodynamics of rare earth elements in liquid iron. *J. Less Common Metals* **110**, 187–193 (1985).
- Li, W. C. Thermodynamics of the formation of rare earth inclusions in steel. *Iron and Steel* **21**, 7–12 (1986).
- Byun, J., Shim, J., Cho, Y. & Lee, D. Non-metallic inclusion and intragranular nucleation of ferrite in Ti-killed C–Mn steel. *Acta Metall.* **51**, 1593–1606 (2003).
- Yang, J., Yamasaki, T. & Kuwabara, M. Behavior of inclusions in deoxidation process of molten steel with *in situ* produced Mg vapor. *ISIJ Int.* **47**, 699–708 (2007).
- Seo, C. *et al.* Modification and minimization of spinel ( $\text{Al}_2\text{O}_3\text{-xMgO}$ ) inclusions formed in Ti-added steel melts. *Metall. Mater. Trans. B* **41**, 790–797 (2010).
- Su, Y. *et al.* Photoelectric characteristics of natural pigments self-assembly fabricated on  $\text{TiO}_2/\text{FTO}$  substrate. *J. Nanosci. Nanotechnol.* **9**, 960–964 (2009).
- Wagner, C. *Thermodynamics of alloys* (Massachusetts: Addison-Wesley Press). p. 22 (1952).
- Lupis, C. H. *Chemical thermodynamics of materials* (Amsterdam: North-Holland). p. 31 (1983).
- Liu, Y. H., Lin, Q. & Ye, W. Behavior of rare earths in ultralow sulfur microalloyed steel. *J. Rare Earths* **17**, 207–212 (1999).
- Wang, L. M. *et al.* Thermodynamics and application of rare earth elements in steel. *J. Chin. RE Soc.* **21**, 251–254 (2003).
- Chen, J. X. *Handbook of common datas and graph in steelmaking* (Beijing: Metallurgical Industry Press). p. 757–761 (2010).
- Katsumata, A. & Todoroki, H. Effect of rare earth metal on inclusion composition in molten stainless steel. *Iron Steelmaker* **29**, 51–57 (2002).
- Vahed, A. & Kayd, A. R. Thermodynamics of rare earths in steelmaking. *Metall. Mater. Trans. B* **7**, 375–383 (1976).
- Wang, G. C. *et al.* Experimental and thermodynamic study on formation of inclusions containing cerium in HP295 steel. *J. Chin. RE Soc.* **31**, 161–168 (2013).
- Ono, H. *et al.* Formation conditions of  $\text{Mg}_2\text{TiO}_4$  and  $\text{MgAl}_2\text{O}_4$  in Ti–Mg–Al complex deoxidation of molten iron. *ISIJ Int.* **49**, 957–964 (2009).

28. Tomita, Y. Effect of desulphurization and calcium treatments on the inclusion morphology of 0.4 C-Cr-Mo-Ni steel. *J. Mater. Sci.* **29**, 2873–2878 (1994).
29. Hu, Z. Y. *et al.* Effect of Ce addition on inclusion and microstructure in C-Mn steel. *Metal. Int.* **17**, 11–17 (2012).
30. Wang, L. M., Du, T. & Wu, Y. M. Thermodynamic study on formation RES and RE<sub>2</sub>S<sub>3</sub> between rare earth elements and sulphur in iron-based solution. *J. Chin. RE Soc.* **6**, 11 (1987).

### Acknowledgements

Our work is sponsored by China Steel Company, National Science Council (MOST104-2622-8-006-001) and Research Center for Energy Technology and Strategy (D105-23008) National Cheng Kung University in Taiwan. Thanks Dr. Ho-Lin Tsai, James Augusto, Shuo-Yen Fang and Guan-Ping Qi for their kind help.

### Author Contributions

This paper was proposed by W.-S.H., F.P. and J.Z. contributed to this article equally. This manuscript was written by F.P. The thermodynamic calculations were carried out by F.P. and J.Z. H.-L.C. and Y.-H.S. contributed to data analysis. Y.-H.S. gave us a lot of suggestions to promote our research. All authors reviewed the manuscript.

### Additional Information

**Competing financial interests:** The authors declare no competing financial interests.

**How to cite this article:** Pan, F. *et al.* Thermodynamic Calculation among Cerium, Oxygen, and Sulfur in Liquid Iron. *Sci. Rep.* **6**, 35843; doi: 10.1038/srep35843 (2016).



This work is licensed under a Creative Commons Attribution 4.0 International License. The images or other third party material in this article are included in the article's Creative Commons license, unless indicated otherwise in the credit line; if the material is not included under the Creative Commons license, users will need to obtain permission from the license holder to reproduce the material. To view a copy of this license, visit <http://creativecommons.org/licenses/by/4.0/>

© The Author(s) 2016